



LAWRENCE
LIVERMORE
NATIONAL
LABORATORY

Testing Diamond Strength At High Pressure

K. O. Mikaelian

November 10, 2010

Diamond and Related Materials

Disclaimer

This document was prepared as an account of work sponsored by an agency of the United States government. Neither the United States government nor Lawrence Livermore National Security, LLC, nor any of their employees makes any warranty, expressed or implied, or assumes any legal liability or responsibility for the accuracy, completeness, or usefulness of any information, apparatus, product, or process disclosed, or represents that its use would not infringe privately owned rights. Reference herein to any specific commercial product, process, or service by trade name, trademark, manufacturer, or otherwise does not necessarily constitute or imply its endorsement, recommendation, or favoring by the United States government or Lawrence Livermore National Security, LLC. The views and opinions of authors expressed herein do not necessarily state or reflect those of the United States government or Lawrence Livermore National Security, LLC, and shall not be used for advertising or product endorsement purposes.

Testing diamond strength at high pressure

Karnig O. Mikaelian

Lawrence Livermore National Laboratory, Livermore, California 94551

We present a design to measure the strength of diamond near 30 Mb using the Rayleigh-Taylor instability. It is a variation on the recently proposed design (Mikaelian, Phys. Plas. **17**, 092701 (2010)) using the ignition pulse. To overcome the low opacity of diamond we introduce behind it a high-Z marker, gold, which has relatively large perturbations. The strong diamond acts as a pusher and at wavelengths of 50 μm it flattens out the perturbation; with less or no strength the perturbations grow exceedingly large.

PACS numbers 62.20.F-, 62.50.-p, 47.20.Ma

Diamond is known as one of the strongest materials at atmospheric pressure. Its properties at high pressures, relevant for several applications¹ (planetary cores, etc.) continue to be studied experimentally and theoretically. Recently, a model for diamond strength at high pressures was proposed based on experiments, simulations, and theory.² In this brief communication we propose a new experimental technique to measure the strength of diamond at much higher pressures.

Experiments^{3,4} have measured total stress, up to 8-10 Mb, by analyzing the free-surface velocity of an isentropically compressed diamond sample and extracting the diamond strength. This technique is necessarily one-dimensional in space (1D), using

VISAR⁵ to accurately record the free-surface velocity as a function of time and back-integrating to deduce density and total stress in the sample. Under certain assumptions, one divides total stress into a longitudinal and transverse part, the difference between them being proportional to the yield strength.^{3,4}

In this brief communication we propose another, perhaps more direct determination of diamond strength at high pressures, up to 30 Mb, building upon a method proposed recently.⁶ This method is necessarily two-dimensional in space (2D) and based on the Rayleigh-Taylor (RT) instability as originally proposed by Barnes *et al*.⁷ Upon acceleration, the instability moves material from thin regions making them even thinner to thick regions making them even thicker, and the increased contrast (measured by an x-ray radiograph) between those two regions reveals how much mass has transferred and hence the effect of the instability. Strength reduces this instability. Without going into any detail as to how this is accomplished on a laser system,⁸ we should recall that this method depends on resolving relatively short wavelengths and on identifying strength as the true source suppressing growth. Rather than viewing one method as superior to the other, we should consider them as complimentary.

In addition to its application in the study of planetary interiors¹, diamond is a candidate as an ablator in Inertial Confinement Fusion (ICF) capsules⁹ and its strength, before it melts, is expected to suppress at least partially the growth of RT instabilities. As in Ref. 6, we will continue using the early part of an ignition pulse to drive a planar target with 2D perturbations; these perturbations grow or do not grow depending on the weakness or strength of the target.^{6,7} In fact by simply replacing the tantalum in Ref. 6 by diamond, also called High Density Carbon (HDC), keeping everything else the same we obtain a viable design, except for one difficulty discussed below. Furthermore, one

obtains better contrast than tantalum. This is to be expected because HDC is much stronger than Ta and therefore the contrast between growth and no-growth, indicative of weakness and strength, is much more pronounced with HDC. Taking advantage of this contrast one would significantly improve the experiment by imposing wavelengths longer than the $\lambda=25\text{ }\mu\text{m}$ considered earlier: Such a short wavelength was necessary for Ta, based on models of its strength, to obtain a measurable contrast between strength and no-strength cases, shorter wavelengths being more sensitive to strength. With HDC, however, one can go to $50\text{ }\mu\text{m}$ or even $100\text{ }\mu\text{m}$ wavelengths, which are easier to diagnose, and still maintain a good contrast, making the experiment “easier.” By direct numerical simulations with CALE¹⁰ we find that peak-to-valley amplitudes remain below $1\text{ }\mu\text{m}$ with strength-on while the no-strength cases grow to $9.0\text{ }\mu\text{m}$ and $3.4\text{ }\mu\text{m}$ for $\lambda=50\text{ }\mu\text{m}$ and $100\text{ }\mu\text{m}$ respectively.

Of the three methods discussed in Ref. 6 only method C is viable: The diamond starts flat and the perturbed CH acts as a “pusher,” a technique perhaps described best as micro-indentation.⁶ Diamond, even more than tantalum, would be hard to press or machine into a sinusoidal shape.

This design, simply replacing the Ta with HDC, would have been sufficient had it not been for one diagnostic difficulty: HDC is low Z (6) and therefore difficult to radiograph. The design proposed in Ref. 6 can work for practically all high-Z materials (Au, Pb, Mo, etc.) because a face-on radiograph will reveal growth or no growth and therefore be a measure of strength. Diamond is an exception because it is strong yet low-Z, requiring a modification which, we believe, can be applied to all low-Z materials of interest.

The solution is to introduce a high-Z marker layer and use the HDC itself as a “pusher” acting as a flattening agent. Specifically, we add $10\text{ }\mu\text{m}$ of gold with its

perturbed surface behind the flat diamond. This is method B mentioned in Ref. 6 except the strengths are interchanged – A strong flat “pusher”, diamond, pressing and accelerating a curved “pushee”, gold. The density contrast is $18.24/3.51 \sim 5.2$, or Atwood number ~ 0.68 , leading to vigorous RT growth in the absence of strength. With strength, the diamond does not bend and instead flattens out the perturbation in the gold.

The design is shown in Fig. 1. The ablator is again 50 μm of CHBr (this number was misreported as 75 μm in the text of Ref. 6 – it was 50 μm ; The inset in Fig. 1 of Ref. 6 showed the correct dimensions). Next comes 25 μm of CH, as before, and 25 μm of HDC (replacing the 25 μm of Ta), followed by 10 μm of Au as discussed above. The gold is backed by 200 μm of LiF. This was 200 μm of CH earlier; we switched to LiF because it appears to be preferred as a window for VISAR. Needless to say, careful VISAR measurements on the back side of the gold will be necessary to establish the correct 1D motion. The drive is about 2 ns longer than before, climbing to 180 eV, compared with the previous 140 eV. This higher drive produces higher pressures in HDC – about 30 Mb instead of the previous 10 Mb in Ta. We believe this is as high as one can follow the ignition pulse before melting. Better and no doubt longer drives can be designed to take targets to even higher pressures, but for the present we continue to follow the ignition pulse. Fig. 1 shows the radiation drive but we use the photon-frequency-dependent-source that produces this T_r .

The function of the LiF is well-known: To prevent decompression or possibly spall of the gold layer. The role played by the 25 μm CH tamper here and in Ref. 6 may be less obvious. Since we work within the confines of a “given” drive, viz. the ignition pulse, we use the CH to improve the pressure seen by the HDC. Without it the first shock would pass from CHBr directly to the HDC. With the CH, this shock is somewhat weaker and,

much more importantly, is partially reflected back towards the CHBr and then re-reflected towards the HDC, creating a smoother drive on the HDC. It played the same role in Ref. 6 tamping the drive on Ta. Such temporal shaping of shocks works only if the density (more accurately the impedance) of the middle layer, CH, is less than those of the two materials on either side, CHBr and HDC or Ta.

We now turn to the results of 2D simulations with CALE.¹⁰ The upper surface of the gold has sinusoidal perturbations 6 μm peak-to-valley, a sizable fraction of its average 10 μm thickness and easily diagnosed, if desired, before the start of the pulse. What is interesting, of course, is the disappearance of this contrast between the 13 μm thick part and the 7 μm thin part as the drive is turned on and the diamond flattens it out. If the diamond had little or no strength, it itself would bend and wrap around the heavier gold and the perturbations would grow very large. This is shown in Fig. 2 where we plot the peak-to-valley amplitude at the upper surface of the gold as a function of time for three cases labeled ISG (for Improved Steinberhg-Guinan, the strength model² described in the Appendix), ISG/2 where the diamond strength is reduced to half of its ISG value, and 0 meaning no strength. The last grows to 35 μm , ISG/2 grows to a peak of about 10 μm before decreasing back to its original 6 μm , while ISG essentially flattens out to zero. The wavelength is 50 μm .

For longer wavelengths such as $\lambda=100$ μm perturbations grow even if the strength is ISG: From the initial 6 μm to 13 μm by $t=22$ ns. If strength is ISG/2, then the peak-to-valley amplitude grows to 16 μm . With no strength it evolves to 23 μm .

Needless to say, the main player is the diamond strength. For gold, we used a standard SG model for its strength and compared the results with no strength – there was

practically no difference. The reason, of course, is that gold is quite weak and, compared to diamond, it flows almost like a fluid.

The amplitudes displayed in Fig. 2 do not tell the whole story because the backside of the gold also evolves and a face-on radiograph is sensitive to the total ρr of the gold. The rest of the target being low-Z is transparent to radiographic x-rays. Snapshots of the gold (red) section of the target are shown in Fig. 3 at 19 and 22 ns for the three assumptions concerning diamond strength, all starting from the same method B initial configuration shown at $t=0$. The flattening of the gold by the strong (ISG) diamond is quite clear, and the small overshoot at late time, $t=22$ ns, pushes mass to the edges at $x=0$ and 50 mm. The opposite happens with no strength: Mass accumulates at the middle, $x=25$ mm, indicating robust RT growth.

Without strength at 22 ns the contrast in ρr between the center and the edge is 3.1: The central ρr is approximately 23.6 mg/cm^2 versus the edge ρr of about 7.6 mg/cm^2 only. With ISG the ρr 's are 17.1 and 26.6 mg/cm^2 respectively, a contrast of 0.64, almost five times less.

To summarize, the high-pressure strength of a high-Z material like tantalum can be measured by the method described in Ref. 6. The strength of a low-Z material like diamond can be measured by introducing a high-Z and relatively soft marker like gold as illustrated here. In both cases one can bypass having to shape the strong material by using methods B or C as appropriate.

ACKNOWLEDGMENTS

I am grateful to Dan Clark for providing the ignition pulse, a photon-frequency dependent source. This work was performed under the auspices of the U. S. Department of Energy by Lawrence Livermore National Laboratory under Contract DE-AC52-07NA27344.

APPENDIX: THE IMPROVED STEINBERG-GUINAN MODEL

The yield strength Y in the improved Steinberg-Guinan model² (ISG) is given by

$$Y = Y_0[1 + \beta(\varepsilon_0 + \varepsilon_p)]^n \{F[1 + AP(\rho_0 / \rho)^{1/3}] + [1 - F][A_{ISG} + M_{ISG}(\rho / \rho_0)] - B(T - 300)\}$$

where F is a function of the compression ρ/ρ_0 only and given by

$$F = F(\rho / \rho_0) = \frac{1}{1 + e^{\alpha_{ISG}(\frac{\rho}{\rho_0} - \eta_{ISG})}}.$$

There are 4 new parameters, all non-dimensional, in addition to the 8 parameters in the standard Steinberg-Guinan model¹¹ reviewed in the Appendix of Ref. 6 using the same notation.

For diamond we used $Y_0=0.9$ Mb, $\beta=0$, $\varepsilon_0=0$, $n=0.27$, $A=0.44/\text{Mb}$, $\rho_0=3.51$ g/cm³, $B=1.5 \times 10^{-5}/\text{K}$, $Y_{whmx}=10$ Mb, $A_{ISG}=-0.596$, $M_{ISG}=1.588$, $\alpha_{ISG}=3.47$, and $\eta_{ISG}=0.88$.

In the calculations labeled ISG/2 we let $Y_0 \rightarrow Y_0/2$ and $Y_{whmx} \rightarrow Y_{whmx}/2$. This work-hardening maximum plays no role as the strength of the diamond never approaches such a high value. Maximum compressions are approximately 3 and maximum yield

strength in diamond reaches 3.25 Mb with ISG and 1.7 Mb with ISG/2. The maximum pressure, in both cases, was about 30 Mb.

Clearly, the SG model is recovered if $F \rightarrow 1$, for example, by letting $\eta_{ISG} \rightarrow \infty$.

The SG and ISG models for diamond are compared in Fig. 4.

REFERENCES

¹F. D. Stacey, Rep. Prog. Phys. **68**, 341 (2005); M. Koenig, A. Benuzzi-Mounaix, A. Ravasio, T. Vinci, N. Ozaki, S. Lepape, D. Batani, G. Huser, T. Hall, D. Hicks, A. MacKinnon, P. Patel, H.-S. Park, T. Boehly, M. Borghesi, S. Kar, L. Romagnani, Plas. Phys. Control. Fusion **47**, B441 (2005).

²D. Orlikowski, A. A. Correa, E. Schwegler, and J. E. Klepeis, Shock Compression of Condensed Matter, AIP Conference Proceedings **955**, 247 (2007); R. E. Rudd and J. E. Klepeis, J. App. Phys. **104**, 093528 (2008).

³D. K. Bradley, J. H. Eggert, R. F. Smith, S. T. Prisbrey, D. G. Braun, J. Biener, A. V. Hamza, R. E. Rudd, and G. W. Collins, Phys. Rev. Lett. **102**, 075503 (2009).

⁴R. S. McWilliams, J. H. Eggert, D. G. Hicks, D. K. Bradley, P. M. Celliers, D. K. Spaulding, T. R. Boehly, G. W. Collins, and R. Jeanloz, Phys. Rev. B **81**, 014111 (2010).

⁵P. M. Celliers, D. K. Bradley, G. W. Collins, D. G. Hicks, T. R. Boehly, and W. J. Armstrong, Rev. Sci. Instrum. **75**, 4916 (2004).

⁶K. O. Mikaelian, Phys. Plasmas **17**, 092701 (2010).

⁷J. F. Barnes, P. J. Blewett, R. G. McQueen, and K. A. Meyer, J. Appl. Phys. **45**, 727 (1974).

- ⁸H-S. Park, K. T. Lorenz, R. M. Cavallo, S. M. Pollaine, S. T. Prisbrey, R. E. Rudd, R. C. Becker, J. V. Bernier, and B. A. Remington, *Phys. Rev. Lett.* **104**, 135504 (2010); H-S. Park, B. A. Remington, R. C. Becker, J. V. Bernier, R. M. Cavallo, K. T. Lorenz, S. M. Pollaine, S. T. Prisbrey, R. E. Rudd, and N. R. Barton, *Phys. Plasmas* **17**, 056314 (2010).
- ⁹J. Biener, D. D. Ho, C. Wild, E. Woerner, M. M. Biener, B. S. El-dasher, D. G. Hicks, J. H. Eggert, P. M. Celliers, G. W. Collins, N. E. Teslich Jr., B. J. Kozioziemski, S. W. Haan, A. V. Hamza, *Nucl. Fusion* **49**, 112001 (2009) ; D. S. Clark, S. W. Haan, B. A. Hammel, J. D. Salmonson, D. A. Callahan, R. P. J. Town, *Phys. Plasmas* **17**, 052703 (2010).
- ¹⁰R. T. Barton, *Numerical Astrophysics*, edited by J. M. Centrella, J. M. LeBlanc, R. L. Bowers, and J. A. Wheeler (Jones and Bartlett, Boston, 1985); R. E. Tipton, *Megagauss Technology and Pulsed Power Applications*, edited by C. M. Fowler, R. S. Caird, and D. J. Erickson (Plenum Press, New York, 1987).
- ¹¹D. J. Steinberg, S. G. Cochran, and M. W. Guinan, *J. Appl. Phys.* **51**, 1498 (1980).

Figure Captions

Fig. 1. (Color) Target and drive used in the paper. The target consists of 50 μm of CHBr ablator (green), followed by 25 μm of CH tamper (yellow), 25 μm of diamond (blue), 10 μm of gold (red), backed by 200 μm of LiF window (cyan). The RT pulse driving the target is the same as the early, 0-17 ns, part of the ignition pulse, held constant at ~ 180 eV for another half a nanosecond before turning off.

Fig. 2. Time evolution of the peak-to-valley amplitude on the upper surface of the gold driven by flat diamond (See Fig. 3). The strength model ISG is outlined in the Appendix. ISG/2 refers to half this strength, and the fast growing upper curve labeled 0 assumes no strength in the diamond. Gold strength has no effect on these curves. $\lambda = 50 \mu\text{m}$.

Fig. 3. (Color) Snapshots of the CALE calculations at 19 and 22 ns for the three assumptions concerning diamond strength: ISG, ISG/2, and 0. As in Fig. 1, green=CHBr, yellow=CH, blue=diamond, red=gold, and cyan=LiF. The scale is given by the horizontal width, $\lambda = 50 \mu\text{m}$.

Fig. 4. Yield strength of diamond as a function of compression ρ/ρ_0 for the SG and ISG models, evaluated at $T=300\text{K}$.

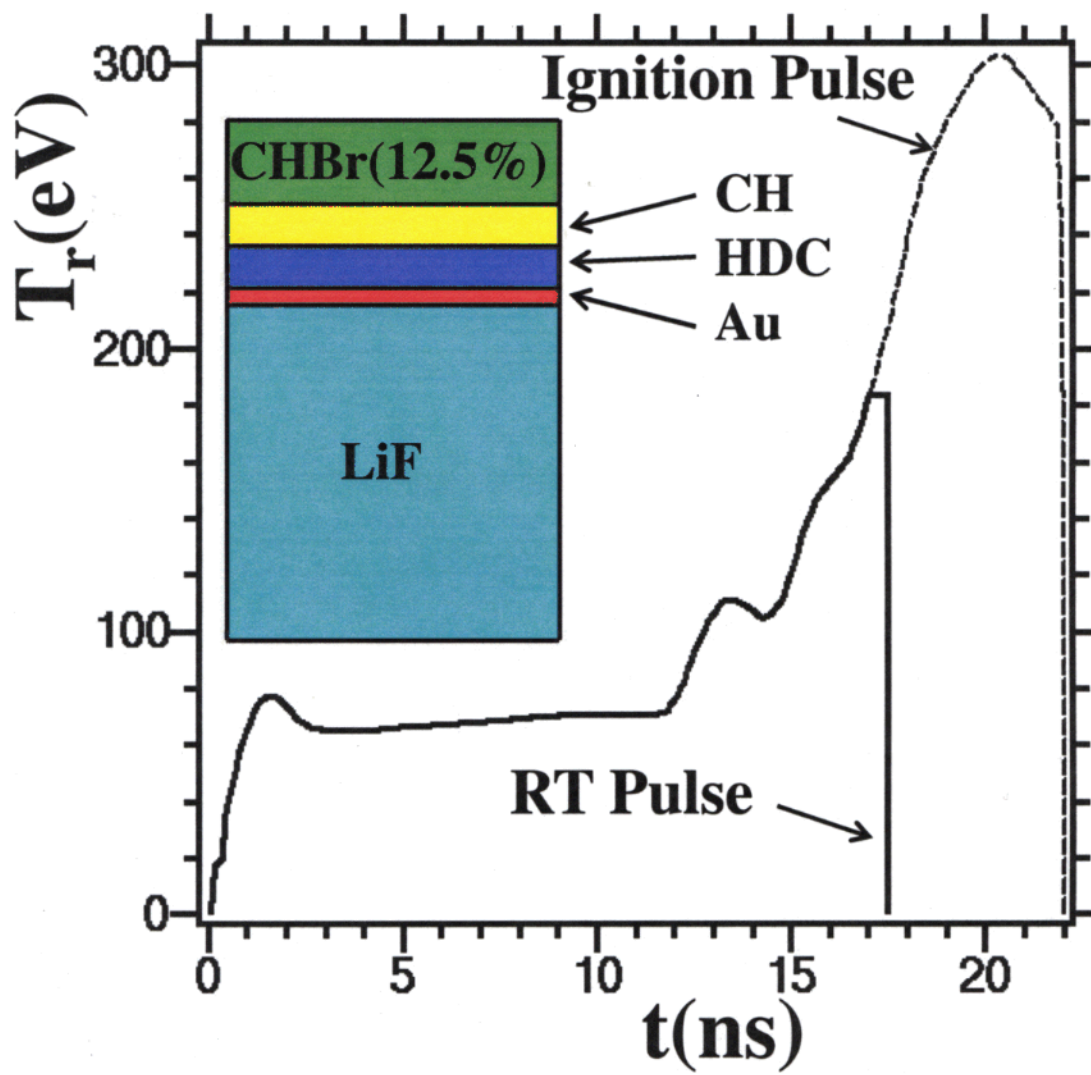


Fig. 1

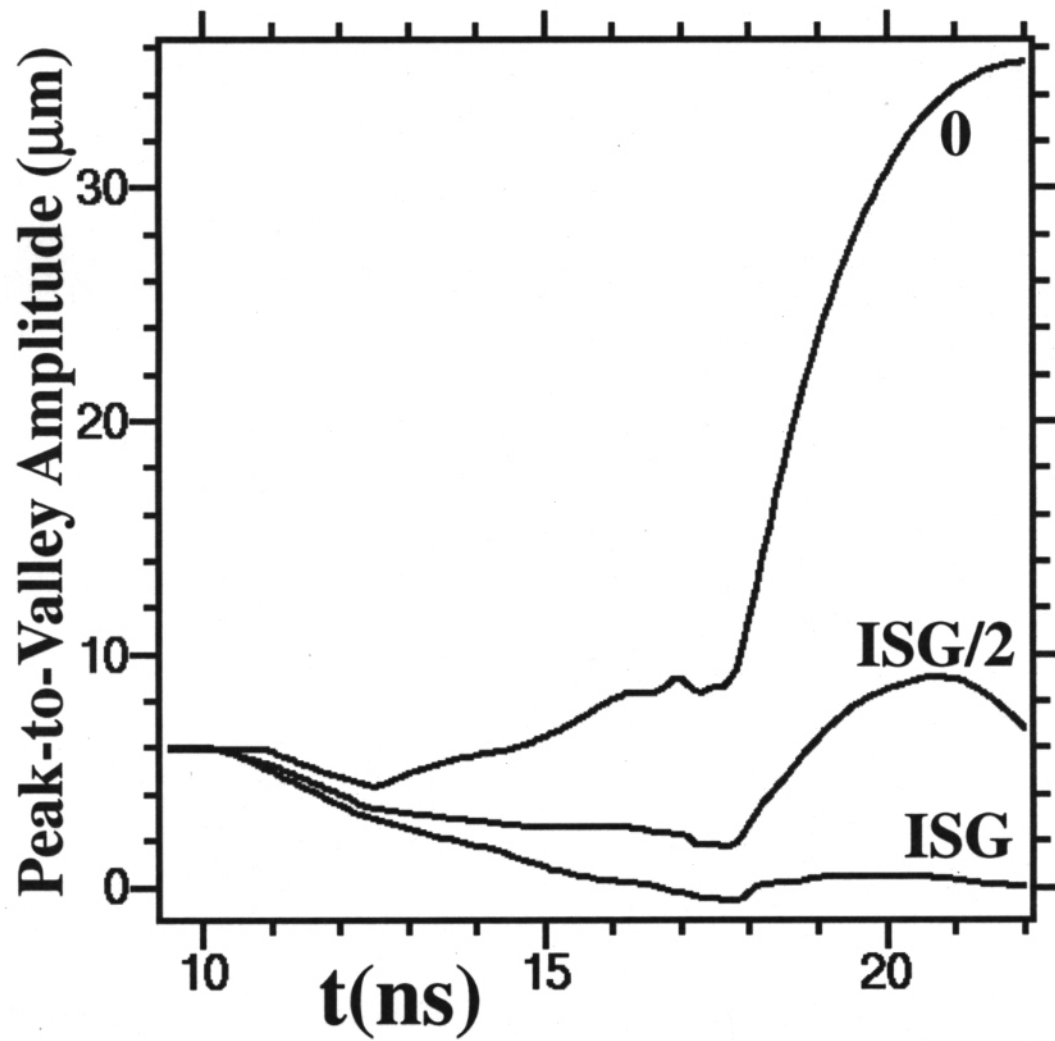


Fig. 2

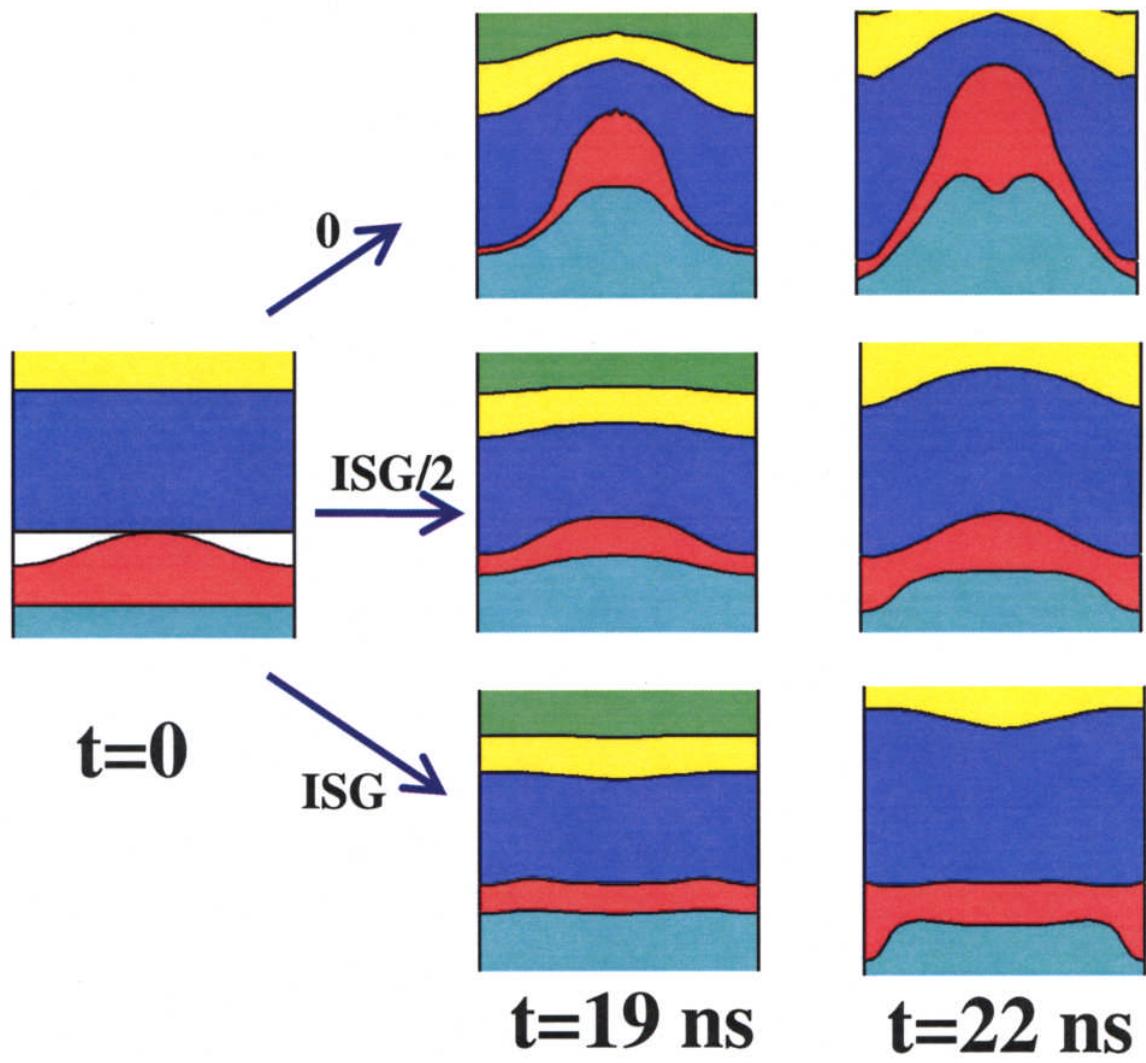


Fig. 3

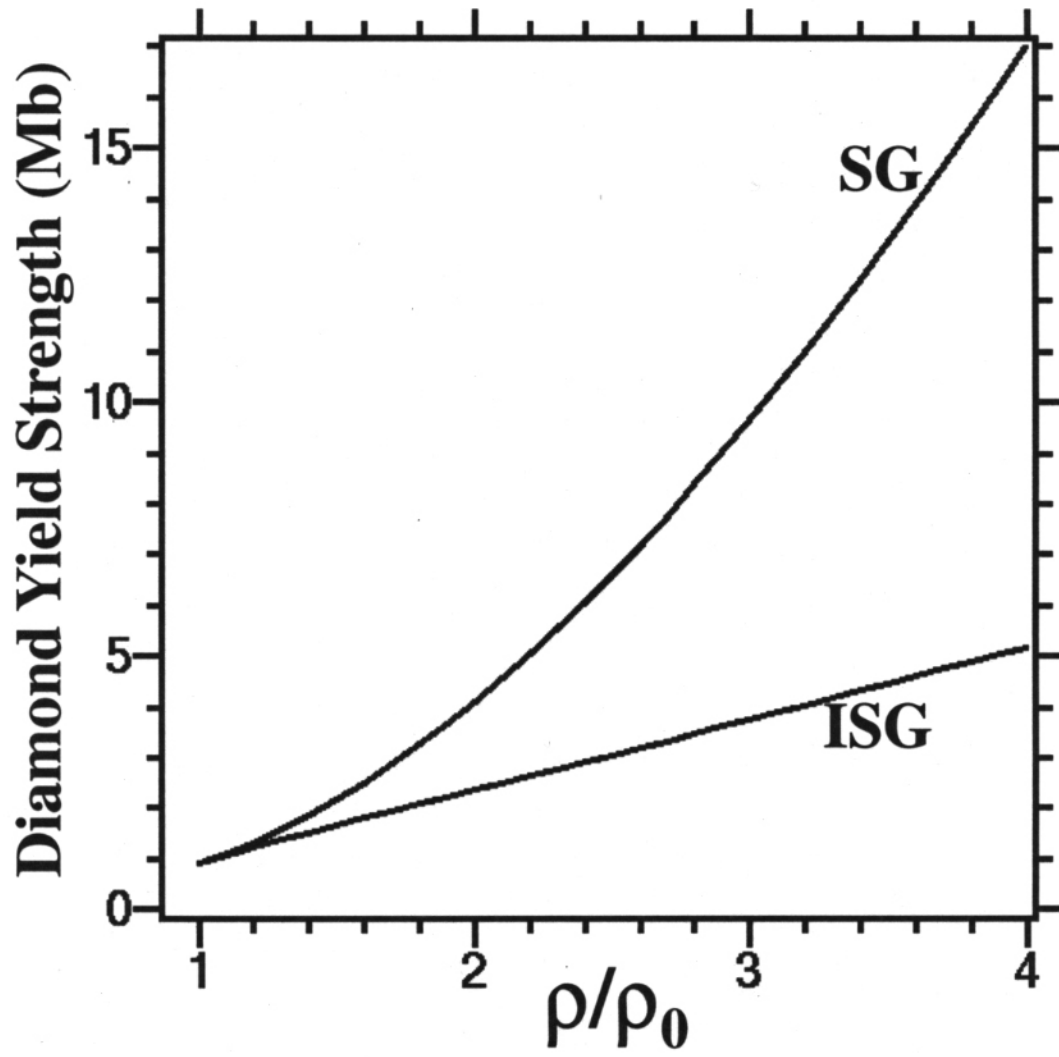


Fig. 4